The Astrophysical Journal, 645:1131–1137, 2006 July 10

ON THE PRIMORDIAL SCENARIO FOR ABUNDANCE VARIATIONS WITHIN GLOBULAR CLUSTERS: THE ISOCHRONE TEST

Maurizio Salaris[1]
Astrophysics Research Institute, Liverpool John Moores University, 12 Quays House, Birkenhead CH41 1LD, UK; and Max Planck Institut für Astrophysik, Karl-Schwarzschild-Strasse 1, Garching D-85748, Germany; ms@astro.livjm.ac.uk

Achim Weiss
Max Planck Institut für Astrophysik, Karl-Schwarzschild-Strasse 1, Garching D-85748, Germany; weiss@mpa-garching.mpg.de

and

Jason W. Ferguson and David J. Fusilier
Physics Department, Wichita State University, Wichita, KS 67260-0032; jason.ferguson@wichita.edu, djfusilier@wichita.edu
Received 2006 January 18; accepted 2006 March 23

ABSTRACT

Self-enrichment processes occurring in the early stages of a globular cluster lifetime are generally invoked to explain the observed CNONaMgAl abundance anticorrelations within individual Galactic globular clusters. We have tested, with fully consistent stellar evolution calculations, whether theoretical isochrones for stars born with the observed abundance anticorrelations satisfy the observational evidence that objects with different degrees of these anomalies lie on essentially identical sequences in the color-magnitude diagram (CMD). To this purpose, we have computed for the first time low-mass stellar models and isochrones with an initial metal mixture that includes the extreme values of the observed abundance anticorrelations and varying initial He mass fractions. Comparisons with "normal" α-enhanced isochrones and suitable Monte Carlo simulations that include photometric errors show that a significant broadening of the CMD sequences occurs only if the helium enhancement is extremely large (in this study, when $Y = 0.35$) in the stars showing anomalous abundances. Stellar luminosity functions up to the red giant branch tip are also very weakly affected, apart from—depending on the He content of the polluting material—the red giant branch bump region. We also study the distribution of stars along the zero-age horizontal branch and derive general constraints on the relative location of objects with and without abundance anomalies along the observed horizontal branches of globular clusters.

Subject headings: globular clusters: general — Hertzsprung-Russell diagram — stars: abundances — stars: evolution — stars: horizontal-branch

1. INTRODUCTION

It was more than 30 years ago that CN variations in the atmospheres of stars within a single globular cluster (GC) were first detected (Osborn 1971). Following this discovery, signs of heterogeneity in the Na (Cohen 1978), Al (Norris et al. 1981), and O (Leep et al. 1986) abundances were also found. Thanks to the large body of spectroscopic data published in the intervening years, it is by now well established that surface abundance variations of C, N, O, Na, and often—but not always, see, e.g., Ramírez & Cohen (2003)—of Mg and Al, exist in stars within individual GCs (see, e.g., the recent review by Gratton et al. [2004]). There is now convincing evidence (e.g., Gratton et al. 2001; Carretta et al. 2005; Cohen & Meléndez 2005) that these elements display a pattern of abundance variations that is very constant all along the red giant branch (RGB) down to the turnoff (TO) region. The pattern shows anticorrelations between CN and ONa (and, when observed, MgAl) superimposed onto a normal α-enhanced heavy-element distribution ($[\alpha/\mathrm{Fe}] \sim 0.3$–0.4) in the sense that negative variations of C and O are accompanied by increased N and Na abundances. The generally accepted hypothesis is that the currently existing stars were born with the observed CNONa abundance patterns. Intermediate-mass asymptotic giant branch (AGB) stars have often been invoked as sources of the necessary heavy-element pollution (see, e.g., Ventura et al. 2001; Carretta et al. 2005 and references therein). The envelopes of these AGB stars are expected to show a pattern of CNONa anticorrelations similar to that observed and are expelled after a time of order $\approx 10^8$ yr during the thermal pulse phase. Provided that a significant fraction of the material is not lost from the GC, new stars can form directly out of this matter or from preexisting matter polluted to varying degrees by the AGB ejecta. The iron abundances would be constant among the different subpopulations, as is actually observed (see, e.g., Suntzeff 1993).

If this scenario is correct, the observed abundance anomalies contain valuable information about the early stages of GC formation and evolution. Current AGB stellar models are not yet able to give a definitive quantitative prediction of the element abundances in the envelopes of intermediate-mass AGB stars due to a number of theoretical uncertainties (see, e.g., Ventura & D'Antona 2005), but it is well established that matter polluted by AGB stars has to show an He enrichment with respect to the original cluster chemical composition. An alternative scenario invokes pollution from mass lost from evolved RGB stars that experienced extra-deep mixing (Denissenkov & Weiss 2004). The expelled matter would not be He-enhanced in this case.

In this paper we assess if theoretical stellar isochrones representative of stars born out of matter showing the observed abundance anomalies are compatible with the narrow sequences traced

[1] Guest User, Canadian Astronomy Data Centre, which is operated by the Dominion Astrophysical Observatory for the National Research Council of Canada's Herzberg Institute of Astrophysics.

by the observed broadband CMDs of most of the Galactic GCs—where stars with different degrees of these anticorrelations lie on essentially identical sequences—and their luminosity functions. This test has not been performed in a fully consistent manner until now. Only D'Antona et al. (2002) have addressed the issue, but they investigated the effect of an increased helium abundance only at constant Z. In our analysis we have computed models, isochrones, and luminosity functions of stellar populations born with both a normal α-enhanced heavy-element mixture and, for the first time, with a metal distribution displaying typical extreme values of the observed CNONa anticorrelations. As a further step, we also investigate if the theoretical interpretation of the observed CMDs and star counts can help us to discriminate between the AGB and RGB pollution scenarios.

In § 2 we briefly describe the models, while § 3 analyzes the results. Conclusions and considerations about the effect on the models of the MgAl anticorrelation follow in § 4.

2. THE MODELS

We have computed sets of stellar models, theoretical isochrones, and zero-age horizontal branch (ZAHB) sequences for $[\mathrm{Fe/H}] = -1.6$, a representative GC metallicity, appropriate for clusters like M3, M13, and NGC 6752 (according to the Zinn & West [1984] [Fe/H] scale) that all display the CNONa abundance anomalies (see, e.g., Carretta et al. 2005 for NGC 6752; Sneden et al. 2004, Cohen & Meléndez 2005, Johnson et al. 2005 for M3 and M13). We have employed the same stellar evolution code as in Salaris & Weiss (1998) and the same sources for input physics, with exception of the low-temperature opacities, for which we rely on the code and database of Ferguson et al. (2005) instead of Alexander & Ferguson (1994). The "reference" metal abundance distribution is the α-enhanced one by Salaris & Weiss (1998), with $\langle[\alpha/\mathrm{Fe}]\rangle = 0.4$. Our reference models and isochrones employ this heavy-element mixture, $Y = 0.25$ (appropriate for GCs, see, e.g., Salaris et al. 2004) and $Z = 0.001$. We have then considered a second metal mixture, with typical mean abundances of the extreme CNONa anticorrelations, based on the results summarized in Carretta et al. (2005). Assuming that both the CN and NaO anticorrelations are present at the same time in a given star (see, e.g., Table 1 in Carretta et al. 2005), we have modified the reference α-enhanced mixture by an 1.8 dex increase of N, an 0.6 dex decrease of C, an 0.8 dex increase of Na, and an 0.8 dex decrease of O. To fully take into account the effect of this modified or "extreme" mixture in our models, stellar opacity tables have been specifically computed for this investigation. For temperatures higher than 10,000 K we used the tabulations produced with the OPAL online facility[2] that are consistent with their counterpart for the reference mixture. For lower temperatures, appropriate tables were computed with the code presented by Ferguson et al. (2005). Models and isochrones account for this extreme mixture in both the nuclear network and opacities (the effect of metals on the equation of state in the GC metallicity range is negligible; therefore, we used the same tables in both our sets of models). They have $Z = 0.0018$ and two different values of the initial He abundance, $Y = 0.25$ and 0.29. This latter value is taken as representative of the enhanced He abundance in the matter processed by contaminating AGB stars (see D'Antona et al. 2002). The value of Z has been chosen to obtain the same [Fe/H] as in the reference case (changing Y from 0.25 to 0.29 at fixed Z changes the corresponding [Fe/H] by only 0.02 dex so that no adjustment of Z for taking into account the enhanced Y is necessary). As the Fe abundance is kept equal to the reference mixture, the sum (C + N + O) is about 0.3 dex larger by number, a value consistent with the results of Carretta et al. (2005) for the extreme values of the anticorrelations. As a third case that is discussed separately, we also explored the possibility of a much larger Y value for the extreme mixture, by computing a set of models, isochrones and ZAHBs with $Y = 0.35$.

[2] See http://www-phys.llnl.gov/Research/OPAL/new.html.

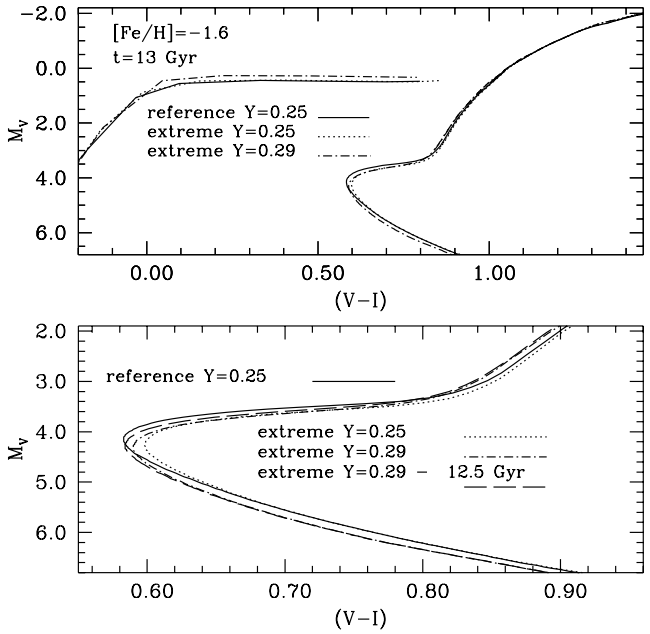

FIG. 1.—CMD of 13 Gyr old isochrones with the reference and extreme metal mixtures, $[\mathrm{Fe/H}] = -1.6$, and the labeled values of Y.

Luminosities and effective temperatures of the isochrones for the two metal mixtures have been transformed into magnitudes and colors using in both cases the α-enhanced color transformations by Cassisi et al. (2004) for $[\mathrm{Fe/H}] = -1.6$. These transformations are, in principle, not adequate for the extreme mixture; however, if comparisons are performed in the $V-(V-I)$ plane, the inconsistency is minimized because $(V-I)-T_{\mathrm{eff}}$ transformations are to a good approximation independent of the metals and their distribution (e.g., Alonso et al. 1996, 1999; Cassisi et al. 2004). We have verified this point by applying to our extreme isochrones and ZAHBs color transformations corresponding to a metallicity increased by a factor of 3 (a factor larger than the difference in the global metal content between the reference and extreme isochrones) with respect to the reference value discussed above. The net result is that the M_V of both isochrones and ZAHBs is shifted by the same—negligible—amount of 0.017 mag. The $(V-I)$ colors are unchanged.

3. RESULTS AND DISCUSSION

The top panel of Figure 1 compares a set of 13 Gyr old, $[\mathrm{Fe/H}] = -1.6$ isochrones from the main sequence (MS) to the tip of the RGB, plus the corresponding ZAHB sequence, for the three different chemical compositions. Notice the complete overlap of the RGB sequences for the reference mixture and the two isochrones with the extreme CNONa anticorrelation and differing initial He mass fractions. This fully satisfies the strong constraint posed by the very narrow RGB sequences in the observed CMDs. Although the He core mass at the He flash is slightly lower for the extreme mixture with $Y = 0.25$ (0.483 vs. 0.490 $M_\odot$ for the reference case; the envelope He mass fraction after the first dredge-up is $Y = 0.262$ in both cases), the ZAHB level is about

0.02 mag brighter. This is due to the higher value of the sum (C + N + O) in the extreme mixture. The extreme mixture with $Y = 0.29$ produces a ZAHB about 0.16 mag brighter than the $Y = 0.25$ case. Along the MS the $Y = 0.29$ extreme isochrone differs in color by only ~0.02 mag from the reference one. The extreme mixture with $Y = 0.25$ instead produces an MS in complete agreement with the reference case. The bottom panel of Figure 1 enlarges the MS, TO, and subgiant branch (SGB) region of the isochrones and displays an additional line corresponding to the extreme mixture, $Y = 0.29$, and an age of 12.5 Gyr. Thereby, we consider a slightly younger age for the anomalous subpopulation. Results analogous to what is described in the following are obtained even if the age of this subpopulation is closer to 13 Gyr. The younger age obviously has no effect on the RGB and ZAHB location. If AGB stars are the main polluters, the most appropriate counterpart of a subpopulation showing the extreme CNONa anticorrelation is likely to be the 12.5 Gyr old isochrone with $Y = 0.29$. In this case the TO has the same color as the reference case and is underluminous by ~0.15 mag.

To check if these small differences along the MS and TO are compatible with the observed CMDs, we made the following experiment. Using a Monte Carlo algorithm, we have populated both the 13 Gyr old reference isochrone and the $Y = 0.29$, 12.5 Gyr old one with the extreme mixture, using a Salpeter (1955) initial mass function and the same number of objects. The individual magnitudes and colors have been then perturbed by a Gaussian (extremely small) 1 σ photometric error of 0.005 mag in both V and I. This photometric error is equal to the mean error in the extremely accurate VI photometries of a large sample of GCs by Stetson (2000).[3]

The result of the simulation is displayed in Figure 2. Even with such a small photometric error, stars with the reference and extreme mixture show a large overlap along the MS and are completely coincident in the TO region and along the RGB (the upper RGB is not displayed, since already from Figure 1 one can notice that reference and extreme isochrones with both $Y = 0.25$ and 0.29 overlap completely). One has also to take into account that this is a somewhat extreme case, given that stars in real clusters show a range of compositions (and maybe ages?) between these two extreme cases.

The bottom panels of Figure 2 show how the luminosity function (with magnitude bins of 0.10 mag, typical of the best observational counterparts) obtained from the combined 50% reference + 50% extreme population compares to the case of a cluster made of stars all formed out of the reference mixture. The two luminosity functions are essentially identical in shape, apart from minute differences in the TO region. The location and shape of the RGB bump is unchanged.

In the case in which the chemical composition of the polluting matter has $Y = 0.25$, Figure 2 shows the same Monte Carlo simulation as discussed for the case with $Y = 0.29$ (the age for the isochrone with the extreme composition is again 12.5 Gyr). Apart from the identical MS, ZAHB, and RGB that can be seen in Figure 1, one can notice a largely overlapping TO and SGB region. The luminosity function of the 50% reference + 50% extreme population is again essentially identical to the case of a cluster made of stars all formed with the reference mixture, apart from a small shift (by about 0.10 mag) of the center of the RGB bump region toward fainter M_V.

The behavior of the bump brightness in Figure 2 deserves a brief discussion. It is well known that at fixed age, the bump becomes fainter when the metallicity of the isochrone increases at

[3] Data can be retrieved from http://cadcwww.hia.nrc.ca/standards.

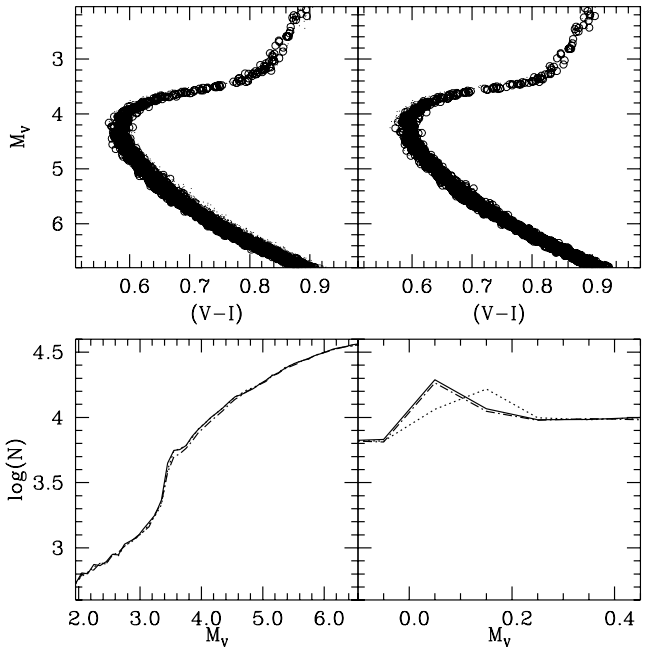

FIG. 2.—CMD of a synthetic GC with [Fe/H] = −1.6. Fifty percent of the cluster stars formed out of the reference mixture and are 13 Gyr old (*dots*); the remaining 50% formed out of the extreme mixture (*open circles*) with either $Y = 0.29$ (*top left*) or $Y = 0.25$ (*top right*) and have an age of 12.5 Gyr. A 1 σ Gaussian photometric error of 0.005 mag is included in the simulation. The bottom panels compare the luminosity functions of these two composite populations (*dotted line*, $Y = 0.25$; *dash-dotted line*, $Y = 0.29$) with the case of a synthetic cluster made only of stars formed out of the reference mixture (*solid line*) for the MS, TO, base of the RGB (*bottom left*), and the RGB bump region (*bottom right*). The star counts are normalized to the same number of stars along the lower MS, with an arbitrary zero point that is different in the two panels.

constant helium, whereas it gets brighter when the initial helium abundance increases at fixed metallicity (see, e.g., Salaris & Cassisi 2005; Cassisi & Salaris 1997; Caloi & D'Antona 2005). Also, the bump feature has a nonnegligible intrinsic width of order 0.2 mag. The center of the bump region in the extreme population with $Y = 0.25$ is fainter than the reference one by ~0.10 mag, due to its higher total metallicity Z (the small age difference between reference and extreme population does not play a major role). In a composite population made of stars with both reference and extreme compositions, the two bump regions overlap partially, due to their intrinsic widths, and their convolution produces a single well-defined feature, as in real GCs (e.g., Zoccali et al. 1999). Different weights of the reference and extreme components will produce different shifts of the magnitude of the composite bump, compared to the reference case. When $Y = 0.29$ for the extreme mixture, the bump center is fainter by only 0.02 mag compared to the reference one, due to the increase of its luminosity produced by the higher initial Y. The composite population will therefore show a bump at essentially the same brightness of the reference isochrone. In general, once the Y value of the extreme population is fixed, both the center and the shape of the resulting composite bump feature are modulated by the relative weights of the two components.

3.1. *The Case of an Extreme Mixture with* $Y = 0.35$

Figure 3 compares the 13 Gyr old reference isochrone and ZAHB, with a 12.5 Gyr old counterpart computed with the extreme mixture and $Y = 0.35$. The differences found for the case of $Y = 0.29$ are, as expected, amplified. The MS below the TO is bluer on average by ~0.05 mag in the extreme isochrone, its TO

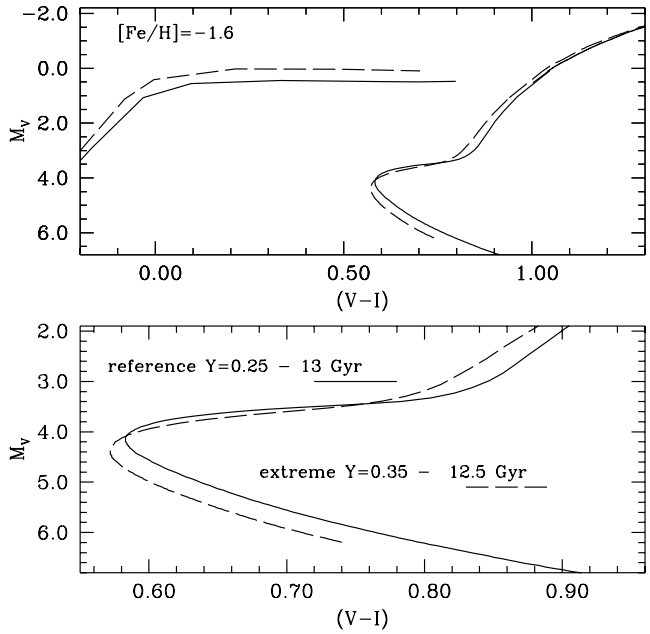

FIG. 3.—Same as Fig. 1, but for the labeled mixtures. The fainter end of the MS in the $Y = 0.35$ isochrone corresponds to a mass of 0.55 $M_{\odot}$.

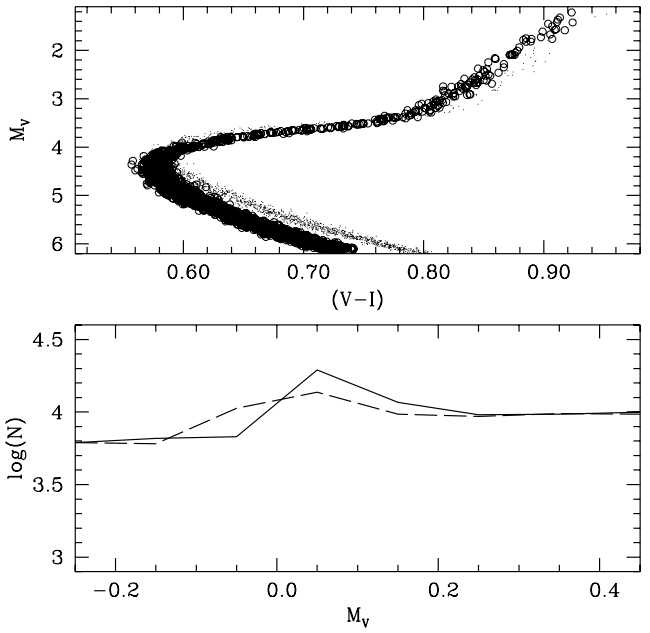

FIG. 4.—CMD of a synthetic GC with $[\mathrm{Fe/H}] = -1.6$ (*top*). Fifty percent of the cluster stars formed out of the reference mixture and are 13 Gyr old (*dots*); the remaining 50% formed out of the extreme mixture (*open circles*) with $Y = 0.35$ and have an age of 12.5 Gyr. A 1 σ Gaussian photometric error of 0.005 mag is included in the simulation. The bottom panel compares the RGB bump region of the luminosity function of this composite population (*dashed line*) with the case of a synthetic cluster made only of stars formed out of the reference mixture (*solid line*). The star counts are normalized to the same number of stars along the lower MS.

is fainter by 0.25 mag (and bluer by 0.01 mag), and the lower RGB is bluer by ~0.03 mag, this latter difference being almost zero in the upper part of the RGB. The ZAHB is brighter by ~0.45 mag compared to the reference mixture.

Figure 4 displays a synthetic CMD of a composite population similar to the case discussed above. Fifty percent of the cluster stars formed out of the reference mixture and are 13 Gyr old (*dots*); the remaining 50% formed out of the extreme mixture (*open circles*) with $Y = 0.35$ and have an age of 12.5 Gyr. A 1 σ Gaussian photometric error of 0.005 mag is included. The MS of the two subpopulations are now clearly separated in the CMD, whereas the TO and SGB regions have a large degree of overlap. The lower RGB of the $Y = 0.35$ subpopulation is also separated from the reference one. We have verified that 1 σ photometric errors of ~0.03 mag in V and I would merge the two MS sequences into a single one. An accurate analysis of the width of the observed MS of individual clusters is necessary to conclusively assess if a component with such a large initial He abundance is present. It is perhaps interesting to notice that subcomponents with very high initial Y have been discovered in one cluster, namely, NGC 2808 (see, e.g., Carretta et al. [2004] for a recent spectroscopic study of the abundance anomalies in this cluster), in addition to the well-known case of ω Centauri, which also shows, however, a spread in [Fe/H] (see, e.g., Suntzeff & Kraft 1996; Norris 2004; Sollima et al. 2005; Piotto et al. 2005 and references therein) not existing in NGC 2808 (e.g., Carretta et al. 2004). D'Antona et al. (2005) found indications of a super He-rich ($Y \sim 0.40$) population from an analysis of the width of its MS.

Figure 4 displays also the RGB bump region of the luminosity function of the composite population described before, compared to the case of a reference isochrone. The center of the bump is displaced toward brighter luminosities by no more than ~0.05 mag. The two bump features show a large overlap and a somewhat different shape. These differences are due to the fact that although the $Y = 0.35$ extreme isochrone produces a bump that is about 0.15 mag brighter than the reference isochrone (due to the much larger initial He abundance), it is also less pronounced (because of the less efficient first dredge-up at this high Y, and smaller discontinuity of the H profile) and still overlaps partially with the bump of the reference population. The convolution of the two bump regions with the 50 : 50 weights produces this composite feature. The rest of the luminosity function shows only minute differences (comparable to the case of the composite mixtures displayed in Fig. 2) around the TO region.

3.2. *Populations along the Horizontal Branch*

A major difference between populations formed out of the reference and extreme mixtures is the ZAHB brightness at colors redder than $(V - I) \sim 0.0$ (see Fig. 1). At bluer colors the ZAHBs become more vertical and tend to overlap. A theoretical prediction of the expected color of the ZAHB (and the whole HB) in the reference and extreme populations is, however, difficult, given the lack of theoretical understanding of the mass-loss processes along the RGB phase. What is generally done is to assume an average amount of mass lost along the RGB (for example, using the Reimers [1975] mass-loss law and choosing appropriately its free parameter η) and a spread around this value that best reproduce the observed color extension of the HB in individual clusters. Here we investigate in the most general way how models with reference and extreme mixtures (both present within clusters showing the abundance anomalies) can coexist along the HB sequence, irrespective of the actual HB morphology in individual clusters.

Figure 5 displays the CMD of nonvariable HB stars in the Galactic GCs M3 and M13 (data from Ferraro et al. [1997] and Stetson [2000], respectively) that both show the abundance anticorrelations discussed in this paper. The HB of M13 has been first shifted in color to account for its slightly different reddening compared to M3 [$E(B - V) = 0.01$ for M3 and $E(B - V) = 0.02$ for M13, following Dutra & Bica 2000] and then in V magnitude

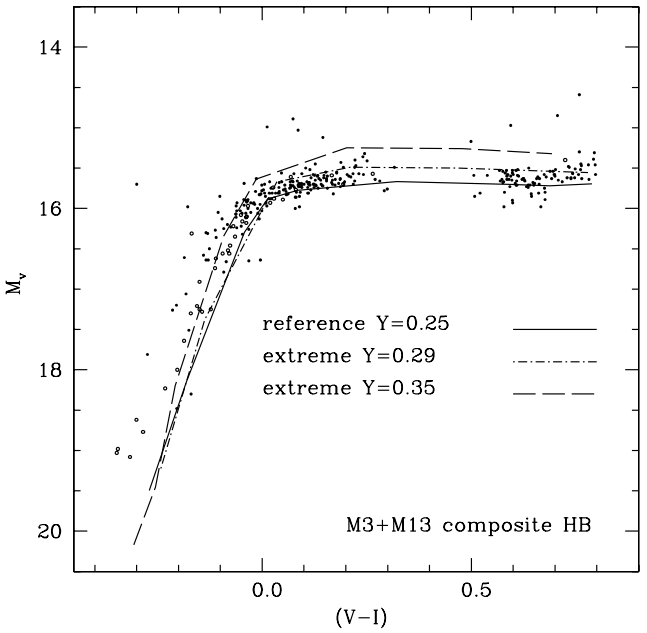

FIG. 5.—CMD of ZAHBs for the labeled chemical compositions, compared to a composite HB obtained combining observations of M3 (*filled circles*) and M13 (*open circles*; see text for details).

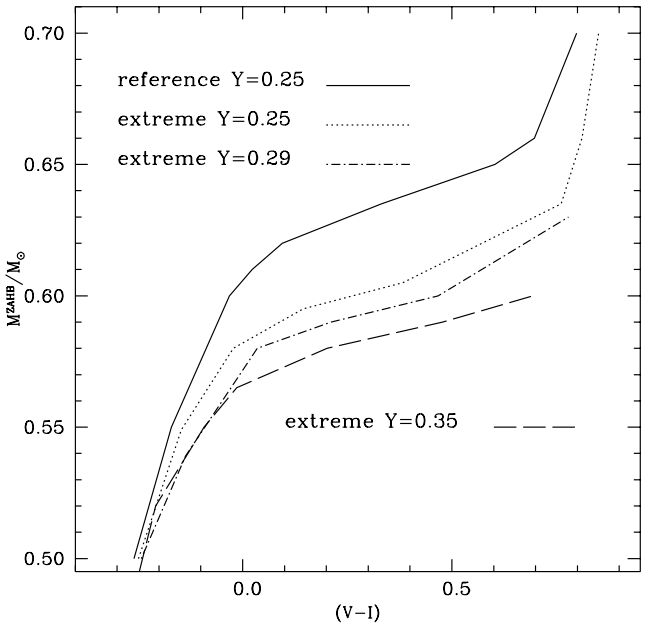

FIG. 6.—Relationship between stellar mass and $(V-I)$ color for ZAHB models with the labeled initial compositions.

until the two HBs overlap along the common blue part. In this way, one obtains an empirical template at the [Fe/H] of the models that covers approximately the whole possible HB color extension [the gap located between $(V-I) \sim 0.3$ and ~ 0.5 corresponds to the RR Lyrae instability strip] and poses as an empirical constraint to the models. The ZAHB for the reference mixture is also plotted, shifted in color to account for the reddening of M3, and shifted in V, until the approximate lower envelope of the observed HB is matched (given that the ZAHB marks the start of the HB phase). To this end we followed the procedure described in Salaris & Weiss (1997). We have looked into the brightness distribution of HB stars in a few color bins along the horizontal part of the observed HB. For each color bin, count histograms for brightness bins were created; the brightness bins were typically 0.05 mag wide (depending on the HB population). We set the ZAHB level to the upper brightness of that bin that shows a decrease in star counts by a factor ≥ 2 and where the brighter bins contain more than 90% of all candidate HB stars under consideration. The ZAHBs for the extreme mixtures with $Y = 0.29$ and 0.35 (the case of $Y = 0.25$ is not shown, given that its ZAHB is essentially identical to the reference one, as already discussed and shown in Fig. 1) are also displayed, after we applied the same color and magnitude shifts employed for the reference ZAHB.

We can now study two different possibilities, in the reasonable assumption that the ZAHB of stars with the reference mixture coincides with the observed one. We consider first the case of an RGB mass loss that populates the three ZAHBs in the horizontal part, where $(V-I) \geq 0$. With this assumption, one can easily notice that the $Y = 0.29$ models are located almost at the upper envelope of the empirical HB and the $Y = 0.35$ one at even brighter magnitudes. This choice for the RGB mass loss of the extreme populations is probably still viable for the $Y = 0.29$ case, but only if the percentage of stars showing the extreme anticorrelation is negligible. In fact, in this case only a few stars of the entire HB population will be evolved above the $Y = 0.29$ ZAHB, therefore not contradicting the evidence of very few objects present above this sequence. The $Y = 0.35$ case appears to be definitely ruled out, because the ZAHB is essentially above the upper limit of the observed data distribution. The case of an extreme mixture with $Y = 0.25$ is still viable, given that the corresponding ZAHB is essentially coincident with the reference one. It is only in the perhaps unrealistic case that the fraction of stars with the reference chemical composition is negligible, that the extreme populations with either $Y = 0.35$ or 0.29 can also be present in this HB color range. In fact, in these conditions it would be the ZAHB of the extreme populations that should be matched to the observed counterpart by applying an additional shift toward fainter magnitudes.

As a second case we consider an RGB mass loss that populates the ZAHBs in the color range $(V-I) < 0.0$. In this case the reference ZAHB and the extreme one with $Y = 0.29$ (the one with $Y = 0.25$ as well) overlap completely and can both coexist without contradiction with the empirical data. When $(V-I)$ is below ~ -0.15 also, the $Y = 0.35$ ZAHB tends to overlap with the others.

A general conclusion of this analysis is that ZAHB objects born out of the reference and extreme (with $Y > 0.25$) mixtures cannot coexist in comparable quantities along the horizontal part of the HB. They can coexist along the bluer HB sequence with the $Y = 0.35$ population being eventually located at $(V-I) < -0.15$. As another possibility they can also coexist if objects with the reference composition occupy the $(V-I) \geq 0$ region (and eventually also the bluer part of the ZAHB), but the extreme populations are located only at $(V-I) < 0.0$. The opposite case looks less feasible. In fact, if the mass loss is such that the $Y = 0.29$ (or 0.35) ZAHB objects populate the observed sequence at $(V-I) \geq 0.0$, the reference ZAHB will tend to be underluminous compared to the observed blue sequence; this is because an additional vertical shift of $\sim +0.2$ or +0.5 mag has to be applied to the reference and extreme ZAHBs displayed in Figure 6 in order for the extreme sequences to match the observed horizontal part of the ZAHB.

In a cluster like M13, whose HB is populated essentially at the blue side, reference, $Y = 0.25$, and $Y = 0.29$ extreme populations can coexist along the whole observed sequence; an eventual $Y = 0.35$ subpopulation can coexist only at the bluer end of

the observed HB. In the case of M3, populated mainly in the horizontal part but also with a tail of objects at $(V-I) < 0.0$, extreme (with $Y = 0.29$ or 0.35) and reference subpopulations can coexist only if the extreme components are located at the blue side of the observed HB.

Figure 6 shows the stellar mass–$(V-I)$ relationship along ZAHBs with four different chemical compositions. For a fixed value of the mass, the ZAHB models with the anticorrelated mixture are generally redder than the reference counterparts. This is due to the increased CNO abundance and lower He core mass. An increase of Y at a fixed metal mixture shifts the ZAHB location of a given mass slightly more to the red. The initial mass of stars evolving at the RGB tip in the reference isochrone (13 Gyr) and in the extreme isochrone with $Y = 0.25$ (12.5 Gyr) is $0.8\,M_{\odot}$; for a 12.5 Gyr old isochrone with the extreme mixture and $Y = 0.29$, the initial value of the evolving mass at the RGB tip is $0.75\,M_{\odot}$, while it is $0.67\,M_{\odot}$ when $Y = 0.35$. These values, combined with the data in Figure 6, predict the minimum amount of mass lost along the RGB, ΔM, to be equal to $\sim 0.18\,M_{\odot}$ for the $Y = 0.29$ isochrone and $\sim 0.14\,M_{\odot}$ for the $Y = 0.35$ isochrone in order to populate the ZAHB at $(V-I) < 0.0$ and < -0.15, respectively.

It may be interesting to analyze the situation if the Reimers (1975) mass-loss law is applied. D'Antona et al. (2002) have also discussed this issue in detail. They assumed that cluster stars showing the CNONa anticorrelation can be well described by isochrones with the same metal mixture of the reference population, an increased initial He mass fraction ($Y = 0.29$), and the same Z. Their results are now to a large extent validated by our analysis. In their analysis they assumed standard values of the mean mass loss along the RGB, obtained from the Reimers (1975) law. The higher He isochrones will then be populated at the bluer part of the HB sequence, the reason for this being the lower initial mass of the stars evolving at the RGB tip. As an example, we applied to our models a Reimers (1975) mass-loss law with a standard $\eta = 0.3$ and obtained an average $\Delta M = 0.175\,M_{\odot}$, which implies an actual mean value of the mass on the reference ZAHB equal to $0.625\,M_{\odot}$. This corresponds to a mean color $(V-I) \sim 0.2$ in the horizontal part of the ZAHB. For a 12.5 Gyr old isochrone with the extreme mixture and $Y = 0.29$, $\Delta M \sim 0.20\,M_{\odot}$ for the same η (it is slightly larger than for the reference isochrone). Under these conditions the corresponding ZAHB would be populated at a mean color $(V-I) \sim -0.1$, given that the mean value of the mass along the ZAHB is $\sim 0.55\,M_{\odot}$. Both reference and extreme subpopulations satisfy one of the conditions described before for their coexistence along the same HB sequence.

4. CONCLUSIONS

In this paper we present for the first time models, isochrones, and ZAHBs consistently computed for a metal mixture with the CNONa abundance anticorrelations observed in Galactic GCs. Our analysis has shown that theoretical CMDs of clusters with abundance anomalies produced by primordial pollution show a significant broadening only if the helium enhancement is extremely large ($Y = 0.35$ in our study) in the stars showing anomalous abundances. Also, stellar luminosity functions from the MS to the RGB tip are essentially unaffected. The spectroscopic results are therefore fully consistent with the theoretical understanding of the photometry. From the photometry alone one cannot decide whether the AGB pollution (increased helium) or the RGB scenario (normal helium) is more likely. Detailed quantitative analyses of the luminosity function in the bump region might give some clues, but only if the fraction of objects with extreme values of the anticorrelations is high. In this case relative shifts of the bump central magnitude of order 0.05–0.10 mag are possible, depending on the amount of initial He in the extreme population and its relative weight compared to the reference component. This kind of relative differences are, however, of the same order of magnitude or smaller than the accuracies of most empirical determinations of the bump brightness (see, e.g., Caloi & D'Antona 2005). It is however intriguing to notice that Caloi & D'Antona (2005) found a variation of 0.14 ± 0.09 in the quantity $\Delta V_{\rm TO}^{\rm bump} = V_{\rm TO} - V_{\rm bump}$ between M3 and M13 (the latter showing the larger value). Assuming the same age and the same [Fe/H] for the two clusters (see, e.g., the discussion in Caloi & D'Antona [2005]), our Monte Carlo simulations of a composite 50 : 50 reference-extreme population discussed above predict an increase of $\Delta V_{\rm TO}^{\rm bump}$ by 0.11 mag (we considered the magnitude of the center of the bump region) when the initial He abundance of the extreme population increases from $Y = 0.25$ to 0.29, and by 0.20 mag, when it goes from $Y = 0.25$ to 0.35. These differences are due to the change of the bump magnitude with changing Y of the extreme population (brighter for increasing Y) but also to the change of the TO brightness of the combined population (fainter for increasing Y of the extreme population, as derived from our composite populations by determining the color distribution of the synthetic MS stars as a function of M_V). A difference in the initial Y abundance for the extreme components of these two clusters (higher Y for M13, which also shows the bluer HB) could explain the difference of the observed $\Delta V_{\rm TO}^{\rm bump}$ values, as also suggested by Caloi & D'Antona (2005).

We have also studied the distribution of stars along the ZAHB and—under the most general assumptions about the mass lost along the RGB phase—derived constraints about the relative location of objects with and without abundance anomalies, along the observed HBs of GCs. Spectroscopic identification of HB objects with abundance anomalies will be decisive in determining the amount of mass lost by their RGB progenitors, on the basis of the location along the HB sequence. Spectroscopy of HB stars might possibly also give some indirect hint of the initial He abundance (hence whether the source of primordial anomalies is pollution from AGB or RGB objects) in stars showing the chemical anomalies. As an example, if sizable samples of HB stars with both reference and extreme metal distribution are coexisting along the horizontal part of the HB of a cluster like M3, this would favor—on the basis of the discussion in § 3—a normal initial He abundance in the stars with extreme composition, hence pollution from RGB stars.

We close with a final comment about the effect of the MgAl anomalies. In our analysis we have neglected the effect of the MgAl anticorrelation (the Al abundance is higher when the Mg content is lower and the Na abundance is higher) observed in several clusters. Its inclusion, however, would not have altered our main results, for the following reasons. Both Al (which is increased at most by ~ 1.0 dex) and Mg (which is decreased by at most ~ 0.4 dex) do not contribute appreciably to the energy generation; therefore, their effect on evolutionary timescales and luminosities is negligible. Along the MS and TO phases a change of Mg and Al does not alter the evolution through opacity effects either, because they do not contribute substantially to the Rosseland opacities in the temperature range that affects the MS location (e.g., Salaris et al. 1993). The He core masses along the RGB evolution are also unaffected (hence also the ZAHB brightness will stay unchanged). As for the RGB color, it is completely determined by the low-temperature opacities (e.g., Salaris et al. 1993);

as a test we have computed low-temperature opacities for a metal mixture with Mg decreased by 0.4 dex and Al increased by 1.0 dex with respect to a reference $[Fe/H] \sim -1.3$–scaled solar metal distribution. Comparisons in the relevant density-temperature range for the appropriate hydrogen abundance show that at the same Fe abundances the two sets of opacities show negligible differences of less than 1%. This means that the MgAl anticorrelation also leaves the RGB location unaffected.

We thank our anonymous referee for comments that helped us to improve the presentation of our results.

REFERENCES

Alexander, D. R., & Ferguson, J. W. 1994, ApJ, 437, 879
Alonso, A., Arribas, S., & Martínez-Roger, C. 1996, A&A, 313, 873
———. 1999, A&AS, 140, 261
Caloi, V., & D'Antona, 2005, A&A, 435, 987
Carretta, E., Bragaglia, A., & Cacciari, C. 2004, ApJ, 610, L25
Carretta, E., Gratton, R. G., Lucatello, S., Bragaglia, A., & Bonifacio, P. 2005, A&A, 433, 597
Cassisi, S., & Salaris, M. 1997, MNRAS, 285, 593
Cassisi, S., Salaris, M., Castelli, F., & Pietrinferni, A. 2004, ApJ, 616, 498
Cohen, J. G. 1978, ApJ, 223, 487
Cohen, J. G., & Meléndez, J. 2005, AJ, 129, 303
D'Antona, F., Bellazzini, M., Caloi, V., Fusi Pecci, F., Galleti, S., & Rood, R. T. 2005, ApJ, 631, 868
D'Antona, F., Caloi, V., Montalbán, J., Ventura, P., & Gratton, R. G. 2002, A&A, 395, 69
Denissenkov, P. A., & Weiss, A. 2004, ApJ, 603, 119
Dutra, C. M., & Bica, E. 2000, A&A, 359, 347
Ferguson, J. W., Alexander, D. R., Allard, F., Barman, T., Bodnarik, J. G., Hauschildt, P. H., Heffner-Wong, A., & Tamanai, A. 2005, ApJ, 623, 585
Ferraro, F. R., Carretta, E., Corsi, C. E., Fusi Pecci, F., Cacciari, C., Buonanno, R., Paltrinieri, B., & Hamilton, D. 1997, A&A, 320, 757
Gratton, R. G., Sneden, C., & Carretta, E. 2004, ARA&A, 42, 385
Gratton, R. G., et al. 2001, A&A, 369, 87
Johnson, C. I., Kraft, R. P., Pilachowski, C. A., Sneden, C., Ivans, I. I., & Benman, G. 2005, PASP, 117, 1308
Leep, E. M., Wallerstein, G., & Oke, J. B. 1986, AJ, 91, 1117
Norris, J. E. 2004, ApJ, 612, L25
Norris, J., Cottrell, P. L., Freeman, K. C., & Da Costa, G. S. 1981, ApJ, 244, 205
Osborn, W. 1971, Observatory, 91, 223
Piotto, G., et al. 2005, ApJ, 621, 777
Ramírez, S. V., & Cohen, J. G. 2003, AJ, 125, 224
Reimers, D. 1975, Mem. Soc. R. Sci. Liege, 8, 369
Salaris, M., & Cassisi, S. 2005, Evolution of Stars and Stellar Populations (New York: Wiley)
Salaris, M., Chieffi, A., & Straniero, O. 1993, ApJ, 414, 580
Salaris, M., Riello, M., Cassisi, S., & Piotto, G. 2004, A&A, 420, 911
Salaris, M., & Weiss, A. 1997, A&A, 327, 107
———. 1998, A&A, 335, 943
Salpeter, E. E. 1955, ApJ, 121, 161
Sneden, C., Kraft, R. P., Guhathakurta, P., Peterson, R. C., & Fulbright, J. P. 2004, AJ, 127, 2162
Sollima, A., Pancino, E., Ferraro, F. R., Bellazzini, M., Straniero, O., & Pasquini, L. 2005, ApJ, 634, 332
Stetson, P. B. 2000, PASP, 112, 925
Suntzeff, N. 1993, in ASP Conf. Ser. 48, The Globular Clusters-Galaxy Connection, ed. G. H. Smith & J. P. Brodie (San Francisco: ASP), 167
Suntzeff, N. B., & Kraft, R. P. 1996, AJ, 111, 1913
Ventura, P., & D'Antona, F. 2005, A&A, 439, 1075
Ventura, P., D'Antona, F., Mazzitelli, I., & Gratton, R. G. 2001, ApJ, 550, L65
Zinn, R., & West, M. J. 1984, ApJS, 55, 45
Zoccali, M., Cassisi, S., Piotto, G., Bono, G., & Salaris, M. 1999, ApJ, 518, L49